Effect of Mold Temperature on the Long-Term Viscoelastic Behavior of Polybutylene Terepthalate

K. Banik,[1] **G. Mennig**[2]
[1] *Institute for Composite Materials (Institut für Verbundwerkstoffe GmbH), Technical, University of Kaiserslautern, D-67663 Kaiserslautern, Germany*

[2] *Institute of Mechanical and Plastics Engineering, Chemnitz University of Technology, D-09107 Chemnitz, Germany*

The effect of mold temperature variation during injection molding on the long-term viscoelastic behavior of polybutylene terepthalate (PBT) was studied by dynamic mechanical thermal analysis (DMTA) and flexural creep tests. The time–temperature superposition (TTS) principle was applied to the experimental data and the master curves were created to predict their long-term behavior. The WLF and Arrhenius models were verified for the shift data in the investigating temperature range and the activation energies for the deformation process were calculated based on the Arrhenius equation. Further a four-element Burger model was applied to the creep results to represent the creep behavior of the PBT processed at two different mold temperatures and to better understand the deformation mechanism. Differential scanning calorimetry (DSC) and density measurements were accomplished to characterize the process-dependent microstructures. POLYM. ENG. SCI., 48:957–965, 2008. © 2008 Society of Plastics Engineers

INTRODUCTION

Polybutylene terepthalate (PBT) is one of the most commercially important polyesters nowadays due to its excellent chemical and heat resistance, rapid crystallization rate compared with the other thermoplastic polyesters and good processability [1]. It is currently utilized in a variety of market segments that include electrical, electronic, automotive, industrial, and chemical sectors. PBT became the subject of interest since the mid-1970s when several groups reported that it could crystallize in different polymorphic forms (see e.g. [2]). Thus most interest has centered on the morphological analysis and the solid-state transition between the alpha and beta crystalline forms in PBT [3–9] which are reported to be reversible and stress-dependent [7, 8]. Although PBT is recognized as one of the important engineering plastics, there has been comparatively less published studies on the long-term viscoelastic properties of this material employing dynamic mechanical measurements and creep tests [10–13]. The present article therefore provides more comprehensive long-term viscoelastic behavior obtained from dynamic and creep data over an extended and continuous range of frequency and temperature.

Polymeric materials being viscoelastic in nature show some of the characteristics of both viscous liquid and elastic solid. Therefore, when polymeric materials are deformed, part of the energy is stored as potential energy and the balance is dissipated as heat. Dynamic mechanical analyzer (DMA) which measures the deformation of a material in response to the sinusoidal stress, has been successfully and effectively used to study the viscoelastic behavior. It usually measures the storage modulus, which indicates the stiffness of the materials, and the mechanical damping. Damping measures the energy lost as heat during the deformation [14]. Since the behavior of polymeric materials is highly dependent on their morphological structures, the dynamic mechanical properties reflect the molecular level changes that occur in a material, when it is subjected to a sinusoidal stress or strain. Under application of such stress or strain over a wide range of temperature, typical molecular changes can pass through three distinct regions associated with different mechanical behaviors. These three regions are (i) the glassy region, yielding high storage modulus (E') and low loss modulus (E''); (ii) the glass-elastomer transition region, shown by significant drop of E' and pronounced E'' peak, and (iii) the flow region, characterized by further drop of E' accompanied by continuous increase in E''. On the other hand, when a polymeric material is subjected to a constant stress, it deforms continuously with time. This time dependent deformation behavior of materials, known as creep, allows better understanding of the relationship between their structure and long-term viscoelastic

Correspondence to: K. Banik; e-mail: kaushik.banik@ge.com
Banik is currently at GE India Technology Center, Bangalore, India.
DOI 10.1002/pen.20989
Published online in Wiley InterScience (www.interscience.wiley.com).

property. The knowledge of the long-term durability of the molded structures is also essential for assessing conditions for the survival time under load. A creep analysis is thus essential if the long-term loading application is to be shown. Research in this direction has showed so far that the long-term deformation behavior of an unreinforced polymer depends strongly on stress, temperature, humidity, void content and crystallinity [15–18].

The viscoelastic properties of polymers are also known to depend on the thermomechanical history during processing, without any chemical intervention. Generally, the commercial molding processes like injection molding, involve three extreme conditions—very high cooling rates, high pressure and shear, and elongational flow while making a polymeric part. Thus the complex thermorheological situations that arise by varying the injection molding process parameters lead to different structural parameters like molecular orientation, residual stress, free volume, and crystallinity (for a semicrystalline polymer) in the finished part varying along the flow as well as along the thickness direction. These can influence the viscoelastic properties of the molding significantly. An extensive review of the effect of processing and more specifically of thermal history on the properties of semicrystalline thermoplastics and its composites has been made by DePorter et al. [19]. From an engineering point of view, the particular process variables that would maximize the product's performance are crucial, where as from a research point of view, the resulting molecular or physical structures that can influence the viscoelastic properties are of fundamental interest.

The aim of this article is to investigate the effect of processing parameters, viz. injection molding temperature on the long-term creep and dynamic loading response and to better understand the phenomena behind the time-dependent changes in the viscoelastic properties.

TIME–TEMPERATURE SUPERPOSITION

Theoretically and experimentally, viscoelastic properties of a polymer, for instance, storage modulus are influenced by both temperature and frequency (or the response time) of the dynamic loading. This seems to imply that the only way to accurately evaluate material performance for a specific application is to test the material under the actual temperature and time conditions that the material will see in the application. But there are often difficulties in attaining the adequate range of temperatures or frequencies in the laboratory conditions for a specific application. Particularly for creep, one of the greatest constraints is the relatively long time required for performing a test. Hence, methods that are able to predict the long-term data have gained considerable attention. A number of observations suggest that the effects of time and temperature are equivalent [20, 21]. It has been widely seen that mechanical behaviors observed after a short time resemble those observed at cooler temperatures. Those observed after a longer time resemble those observed at warmer temperatures. This time–temperature superposition (TTS) is one of the most widely used extrapolation techniques that has been applied to virtually every mechanical property and each kind of plastic [21]. Long-term viscoelastic behavior can be predicted from the short-term test data if the TTS principle is applicable to the studied material. According to the TTS principle, viscoelastic property, $D(t,T)$, at one temperature (T_1) can be related to that at another temperature (T_2) by application of a multiplicative factor, a_T, of the time scale, t, namely,

$$D(t, T_1) = D(t/a_T, T_2) \tag{1}$$

The TTS principle cited above states that the effect of temperature on the time-dependent mechanical behavior is equivalent to a stretching (or shrinking) of the real time for temperatures above (or below) the reference temperature. Practically, data is obtained at wider range of time scales or strain rates experimentally possible, at a range of temperatures. This data can then be shifted by a_T to higher or lower time scales since these are equivalent at higher or lower temperatures; lower temperature experimental data provides information about shorter loading rates and vice versa. The result of shifting data in this way is a master curve of data, which provides a much wider range of information than experimentally possible for the reference temperature.

It is fairly accepted that this superposition manifests itself from the molecular behavior and therefore, equations based on the activation energy (E), such as the Arrhenius equation have been proposed. The Arrhenius equation relates the horizontal shift factor (along the logarithmic time axis) with temperature as

$$\ln a_T = \frac{E}{R}\left[\frac{1}{T} - \frac{1}{T_0}\right] \tag{2}$$

where a_T is the horizontal shift factor, R is the universal gas constant, T_0 is the reference temperature, and T is the experimental temperature. The temperature dependence of the secondary relaxations can generally be described by the Arrhenius equation.

Another commonly used empirical equation for TTS that relates a shift in temperature with a shift in time is the William–Landel–Ferry (WLF) equation:

$$\ln a_T = \frac{C_1(T - T_0)}{C_2 + T - T_0} \tag{3}$$

Here C_1 and C_2 are the constants and T and T_0 are the test and reference temperature, respectively. The WLF equation was found empirically to demonstrate the frequency dependence of glass transition temperature in amorphous substances [20, 22]. It is generally accepted that for the temperature range above the glass transition temperature, shift factor–temperature relationship is very well described by the WLF equation.

 DOI 10.1002/pen

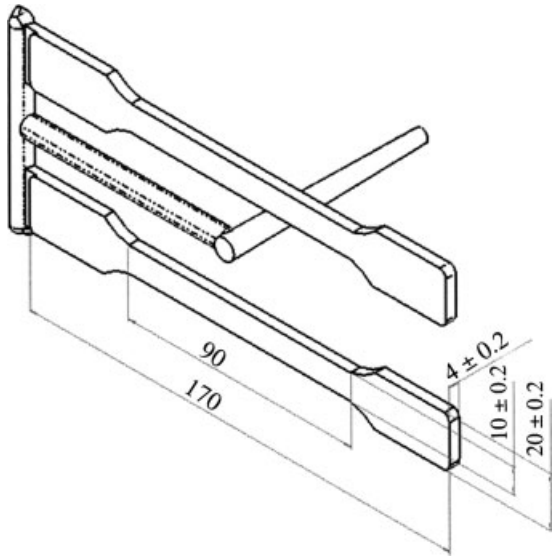

FIG. 1. Schematic of the injection molded specimen (dimensions are in mm).

EXPERIMENTAL

The material used in this study was PBT (Ultradur B 4500 natur) kindly supplied by BASF, Germany. Dumbbell-shaped tensile specimens of 4 mm thickness (see Fig. 1) were produced by injection-molding using Arburg Allrounder 320S (500-350) injection molding machine equipped with a mold temperature controller at two different mold temperatures, viz. 14 and 60°C and are represented by PBT14 and PBT60, respectively. All other processing parameters such as injection flow rate (20 cm^3/s), holding pressure (50 MPa) and holding time (15 s), rest cooling time (25 s), melt temperature (245°C), and pressure-to-switch over (40 MPa) were kept unaltered. Before injection molding, PBT granules were dried at 120°C for 3 h.

Dynamic mechanical tests were performed on a DMA Q800 instrument (TA Instruments, New Castle, USA) in a dual cantilever flexural mode. Specimen with dimensions of ~60 × 10 × 4 mm^3 (length × width × thicknesss) were placed on the test grips inside the sample chamber and then cooled to 0°C. The temperature was allowed to stabilize and then heated at a rate of 3°C min^{-1} until 200°C. The specimens were subjected to a sinusoidal flexural displacement applying a maximum strain of 0.1% which falls within the viscoelastic region at frequencies of 0.1, 1, 5, and 10 Hz. For each frequency, the storage and loss modulus as well as the loss factor were recorded.

Short-time flexural creep tests were performed using three-point bending mode at different temperatures, ranging from 30 to 80°C, in the same DMA Q800 apparatus. In this temperature range, isothermal tests were run on the specimens by increasing the temperature stepwise by 10°C. Prior to the creep measurement, the specimens were equilibrated for 5 min at each temperature and then the flexural creep behavior was tested for 15 min. All the tests with the injection molded PBT were performed under a constant load of 7 MPa, which falls within the linear viscoelastic range determined by checking the proportionality condition [23, 24]. Test specimens of the same dimensions used for dynamic mechanical tests were employed for creep studies and the average of three statistically relevant creep and dynamic mechanical test data has been reported for each kind of specimen.

Differential scanning calorimetry (DSC) was done in a Netzsch 200 DSC instrument (Selb, Germany) to determine the crystallinity of the injection-molded specimens. Calibrations were done using tin and all the scans were performed from 20 to 250°C at a heating rate of 20°C/min by constantly maintaining a nitrogen atmosphere inside the sample chamber. Sample weight of 7–9 mg was employed for each measurement and the amount of crystalline phase was determined by taking the ratio of the heat of fusion of the polymer against the heat of fusion for the 100% crystalline PBT assumed as 145 J/g [25]. The average of three samples was reported for each mold temperature. To determine the effect of thermomechanical history on the crystallinity content of the injection molded specimens, only the first heating scan was taken during thermal analysis.

For a qualitative estimation of the void content (frozen-in free volume) in the injection-molded parts, density measurements were accomplished according to DIN 53479 (procedure A) at ambient temperature in a density measuring instrument provided by the company Sartorius. Ethanol was used for measuring the density of the samples. Then the specific volume was determined from the relation specific volume, $v = 1/\rho$, where ρ is the density of the material. There exists a strong theoretical base relating the specific volume of polymers to the free volume available [26–28]. The advantages of density measurement are that it is comparatively simple and depending upon the process also very small density variation can be dissolved.

RESULTS AND DISCUSSION

Characterization of the Injection Molded Specimens

A calorimetric analysis of the melting process of PBT, presented in Fig. 2, allowed the crystalline phase that was developed due to processing to be identified and quantified. It shows that melting occurs between 227 and 228°C for PBT. An exotherm is observed between 210 and 215°C, which can be identified as recrystallization followed by immediate melting [4]. An additional small exotherm (172–175°C) is also registered for PBT molded at 14°C associated with the melting of small and defective crystals. The DSC determined crystallinity for PBT processed at lower (PBT14) and higher (PBT60) mold temperatures were found to be 28.5 and 31.1%, respectively. While cooling from a higher melt temperature to a lower

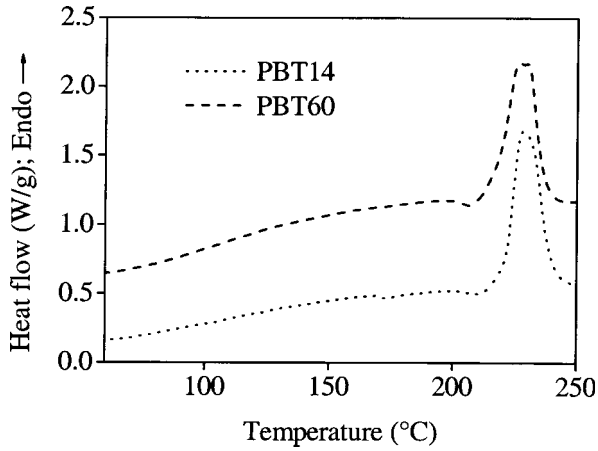

FIG. 2. DSC thermograms of PBT processed at two different mold temperatures.

mold temperature, the polymer passes through the crystallization temperature quicker for a lower mold temperature than for a higher mold temperature. So it gets less time to crystallize. Contrariwise, slower cooling allows the macromolecules to adopt a more regular pattern, forming bigger crystalline areas and resulting in higher crystalline structure. As the temperature gradients during injection molding are very large, so the changes in crystallinity are small. Similar reports are also available in the literature [12, 13].

A change in the injection molding conditions not only affects the crystalline phase, but also the free volume or voids generated in the amorphous phase of the semicrystalline thermoplastics. This can therefore affect the molecular packing density of the finished part. As the deformation behavior of an injection molded part depends strongly on the molecular packing density, so it is important to account for the process-dependent change in free volume. The specific volume determined from the density measurements for PBT14 and PBT60 were found to be 0.7639 and 0.76254 cm^3/g, respectively. This decrease in the specific volume for PBT processed at higher mold temperature is quite significant and can be explained by slower cooling at higher mold temperature that leads to a closer packing of the molecular chains. So less voids or free volume is expected when processed at higher mold temperature.

Dynamic Mechanical Thermal Analysis

Figure 3 represents the dynamic mechanical response of PBT injection molded at 14 and 60°C when subjected to different frequencies ranging from 0.1 to 10 Hz. The plot shows storage modulus (E'), loss modulus (E'') and tan δ as a function of temperature at different frequencies. It shows that storage modulus increases whereas the loss modulus and tan δ (ratio of loss modulus and storage modulus) peak shifts to higher temperature with the increase in frequency as expected. The storage modulus is fairly high at lower temperatures indicating higher stiffness at glassy region and decreases with the increase in temperature as expected. Generally, the tan δ peaks are associated with the transition temperatures [14]. Thus Fig. 3 shows a tan δ peak ~50–54°C corresponding to the glass transition (T_g). The loss modulus also showed pronounced increase near the glass-elastomer transition region. Earlier investigations [10, 29] on the molecular motions of PBT by dynamic mechanical measurements reveal two relaxations. The α relaxation at 50°C (1 Hz) has been ascribed to the micro-Brownian motions of the chains in the amorphous regions whereas the β relaxation at −90°C (1 Hz) involves more restricted motions of the carbonyl group and glycol residue. Chang and Slagowski [13] studied the effect of crystallinity and glass fiber reinforcement on the dynamic mechanical behavior of PBT. They found that the magnitude of α and β relaxation decreases with increasing crystallinity, indicating that the limited motions of the carbonyl and glycol groups occur at least partly in the amorphous regions. Note that the tan δ value (which also represents mechanical damping) is slightly reduced for PBT60 (i.e., with higher crystalline PBT) and T_g shifts to higher temperature for PBT processed at higher mold temperature. This is anticipated as processing at the higher mold temperature or slower cooling rate can lead to a closer packing of the molecular chains with more crystalline phase and less free volume. Hence more energy is required for the segmental mobility to occur. However, the tan δ peak corresponding to the β relaxation cannot be observed in the present study because of the temperature range investigated. Further a slightly higher E' for PBT60 indicates a higher dynamic stiffness resulting from the increase in the crystallinity content [1]. Also, a slightly broader tan δ peak is observed for PBT14 indicating a broader relaxation spectrum for lower mold temperature processed PBT. The results thus demonstrate the fact that the viscoelastic response of polymers is strongly dependent on temperature and thermorheological history during processing.

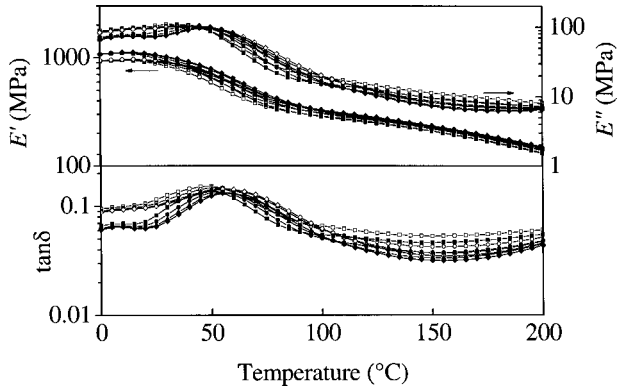

FIG. 3. Effect of temperature and frequency on dynamic storage modulus (E'), loss modulus (E'') and tan δ of PBT molded at 14°C (open symbols) and 60°C (solid symbols); -□-/-■- 0.1 Hz, -○-/-●- 1 Hz, -Δ-/-▲- 5Hz, -◇-/-◆- 10 Hz frequency.

DOI 10.1002/pen

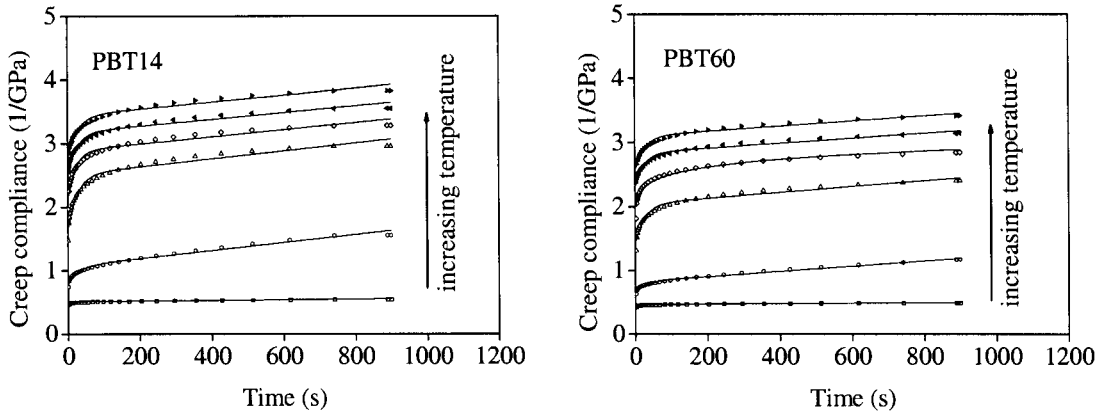

FIG. 4. Creep response of PBT conducted at different temperatures (□ 30°C, ○ 40°C, Δ 50°C, ◇ 60°C, ◀ 70°C, ▶ 80°C).

Moreover, they also suggest that DMTA can be used as a reliable tool for probing the polymer relaxations.

Flexural Creep

The flexural creep behavior of PBT processed at different mold temperature is shown in Fig. 4, where creep compliance is plotted as a function of time at different temperatures ranging from 30 to 80°C. Note that the symbols represent the experimental data and the bold lines represent the model fit (see later). The results show higher creep compliance with increasing temperature for both PBT14 and PBT60. It indicates that an increase in the temperature tends to increase the mobility of the macromolecular chains and hence increase in flexural creep strain or creep compliance. The elastic creep also increased with the temperature. It is clear from the results that PBT specimens molded at higher temperature (PBT60) are more resistant to creep compared with that processed at lower temperature. This difference in creep behavior arises from the difference in the thermal history (cooling rate) that the specimens experience while processing at different mold temperatures. A slower cooling rate at higher mold temperature tends to create more crystalline phase and less free volume that restricts the molecular mobility and is thus manifested by lower creep strain or compliance. The observed creep behavior cannot be accomplished to the difference in frozen-in molecular orientation resulting from processing at different mold temperatures [12].

Prediction of Creep Properties

Generally, linear viscoelasticity is valid for polymer systems that undergo small deformations. On the other hand, nonlinear viscoelasticity is required for modeling large deformations such as those encountered in flowing polymer melts. In linear viscoelasticity, the creep test is often used along with the TTS principle, to explain the behavior of polymeric materials during deformation. It was mentioned earlier that most polymers exhibit a viscous as well as an elastic response to stress and strain. This puts them in the category of viscoelastic materials. Various combinations of elastic and viscous elements have been used to approximate the materials behavior of polymeric melts. Most models are combinations of springs and dashpots—the most common ones are the Maxwell and Kelvin-Voigt models [30].

Burger model is a series of combinations of Maxwell and Kelvin-Voigt models [17, 31] and is shown schematically in Fig. 5. According to this model, the total strain is given by the general equation

$$\varepsilon = \varepsilon_1 + \varepsilon_2 + \varepsilon_3 \tag{4}$$

$$\frac{\varepsilon}{\sigma} = \frac{1}{E_1} + \frac{1}{E_2}(1 - \exp(-tE_2/\eta_2)) + \frac{t}{\eta_1} \tag{5}$$

where ε_1 and ε_2 are the elastic and viscous strain represented by the Maxwell model and ε_3 is the viscoelastic strain represented by Kelvin-Voigt model, E_1 and E_2 are the elastic moduli, η_1 and η_2 represent the viscosity of the material, σ is the applied stress and t is the creep time. The experimental and model plots are shown in Fig. 4 for PBT processed at both the mold temperatures. The first instantaneous deformation arises from the spring or the elastic element (E_1) and later time dependent deformation

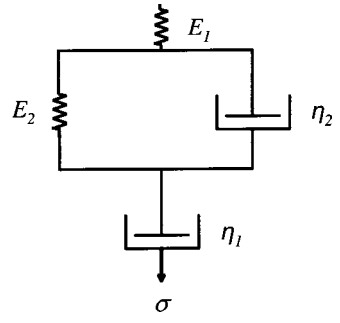

FIG. 5. Schematic of the four-element Burger model.

TABLE 1. Parameters obtained from the Burger model.

Sample	Temperature (°C)	E_1 (GPa)	E_2 (GPa)	η_1 (GPa min)	η_2 (GPa min)
PBT14	30	2.11	28.45	333.33	3.33
	40	1.24	3.87	26.45	2.08
	50	0.61	1.14	26.88	0.52
	60	0.47	1.31	29.76	0.46
	70	0.40	1.47	31.45	0.61
	80	0.36	1.52	30.3	0.7
PBT60	30	2.34	25.56	416.66	3.63
	40	1.51	6.19	40.65	3.03
	50	0.71	1.56	36.23	0.7
	60	0.53	1.58	40.65	0.58
	70	0.44	1.76	42.73	0.7
	80	0.39	1.81	41.66	0.81

comes from the parallel spring and dashpot (η_2) and from the viscous dashpot flow (η_1). The parameters obtained for the model are shown in Table 1. According to this, the modulus (E_1) of the Maxwell spring showed a decreasing function with temperature, which can be attributed to the softening of the material at elevated temperature and the stiffness thus decreased with diminished instantaneous modulus. This indicates that the plastic deformation becomes severe at elevated temperature. The retardant elasticity (E_2) showed a similar dependency on temperature, thus decreasing with increasing temperature. A remarkable drop in viscosity is observed while encompassing from 30 to 40°C. Such a behavior is attributed to the glass transition of PBT as in the glassy state the material is stiffer than in the rubbery state. Hence it shows a significant drop in viscosity when heated above its glassy phase. Also note that the results clearly indicate higher modulus and viscosity of the PBT when it is processed at higher mold temperature. This can be correlated to the microstructure developed in the molded parts. Higher crystallinity as well as molecular packing in the specimens when processed at higher mold temperature of 60°C is expected to show up with an increase in the elastic modulus and viscosity that is manifested during the creep test with reduced tendency to creep. This suggests that the mold temperature during injection molding has a significant effect on the viscoelastic properties of the finished part. However the decrease in viscosity (η_1 and η_2) was found to be rather inconsistent with increasing temperature. This was similar to that reported by Houshyar and Shanks [17], where the viscosity (η_1) varied inconsistently with the increase in fibre content. But nevertheless the results above showed that the Burger model can provide a constitutive representation of the creep behavior of PBT and the modeling parameters provide better insight into the structure-to-property relationship with respect to the change in processing parameters.

Time–Temperature Superposition

An attempt was made to apply the TTS principle to the DMTA data measured in the temperature range of 0–200°C at frequencies of 0.1, 1, 5, and 10 Hz, respectively. The storage moduli data were used to generate master curves for PBT specimens molded at different temperatures. The TA Data Analysis software supplied with the DMA analyzer is capable of performing the TTS procedure for frequency scans. In the generation of the master curve, a reference set of data is chosen. For this study, 30°C was selected as the reference temperature. The remaining sets of data are shifted either to higher or lower frequencies to fall upon the chosen reference. During this superposition, the shift factors are registered. After all of the individual data points are shifted, a single curve, the master curve, is obtained and is displayed in Fig. 6 for PBT processed at both the mold temperatures. It represents a plot of storage modulus as a function of frequency and shows that PBT60 tends to exhibit higher storage modulus, especially at higher frequencies. This is attributable to the higher stiffness resulting from higher crystalline fraction as well as higher molecular packing density in the case of PBT60 that generally tend to stiffen the material and increases its elastic response. The shift factor (a_T) necessary to superimpose the storage modulus data to the reference is different for each temperature and this temperature dependence has been verified by the WLF equation. This has been displayed in Fig. 7.

Rearranging *Eq. 3* gives

$$-\frac{(T-T_0)}{\log a_T} = \frac{C_2}{C_1} + \frac{T-T_0}{C_1} \tag{6}$$

If the shift data obtained from the DMTA measurements follow the WLF equation, then a plot of $-(T - T_0)/\log a_T$ against $(T - T_0)$ is expected to produce a straight line. However, Fig. 7 does not show a linear relationship for PBT molded at different temperatures. A linear relation can be to some extent observed for PBT at temperatures above T_g. A survey of literatures suggests that for the refer-

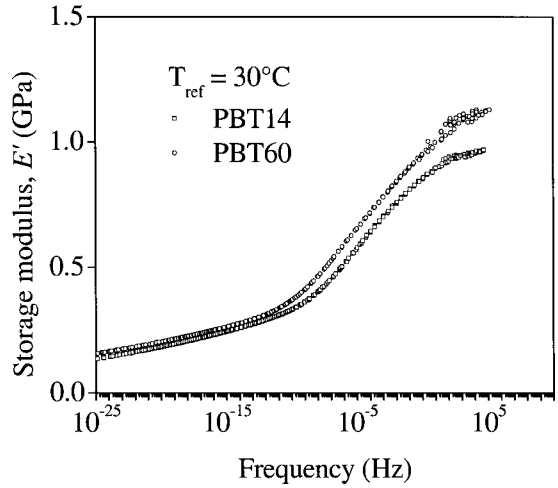

FIG. 6. Storage modulus vs. frequency master curves for PBT at a reference temperature of 30°C.

DOI 10.1002/pen

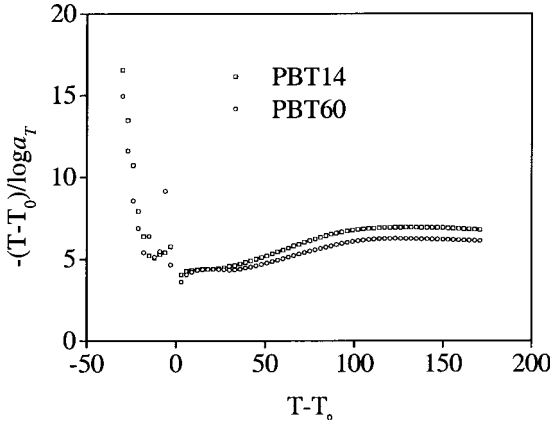

FIG. 7. Plot of $-(T - T_0)/\log a_T$ against $(T - T_0)$ from the DMTA data.

ence temperature above T_g, the shift factor–temperature relationship can be best described by WLF equation [21, 30].

From Fig. 4, it appears that the shapes of the various creep curves can be amenable to the well-known reduction scheme of TTS. Coincidence of the data is good and the master curves (see Fig. 8) show higher creep resistance for PBT molded at higher temperature as anticipated from the short-term creep data. Note that the construction of creep master curves were accomplished by the horizontal shifting of the individual creep curves obtained at different temperatures (see Fig. 4) to the reference temperature (30°C) by using the TA Data Analysis software. Flexural creep compliance at various temperatures is shifted along the logarithmic time scale until the data points overlap creating a master curve. The same procedure has been extensively used by many authors [32–34]. However the master curve generated by shifting the individual creep curves of PBT60 at a reference temperature does not show a continuous creep curve. Generally the master curves are important since the polymer's behavior can be traced over much greater periods of time than those determined experimentally.

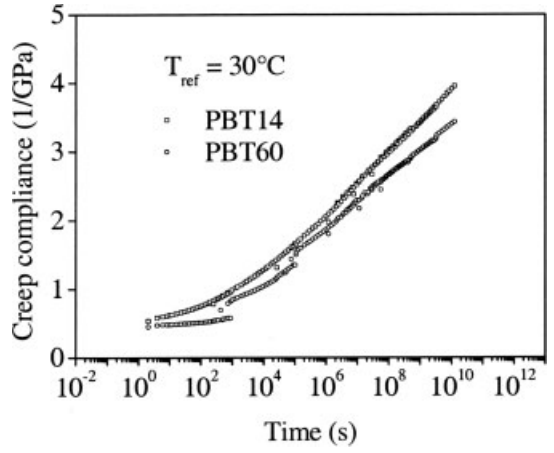

FIG. 8. Creep compliance master curves for PBT; T_{ref} is the reference temperature.

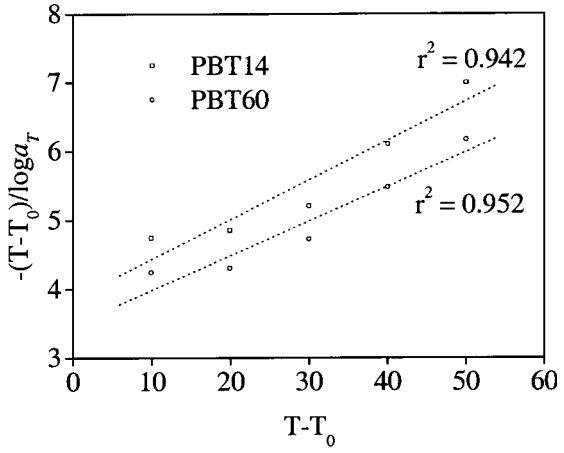

FIG. 9. Plot of $-(T - T_0)/\log a_T$ against $(T - T_0)$ from the creep data; $(\cdots)$ represents first-order regression.

The WLF equation was also tried for the shift factors obtained from the flexural creep data. The results are displayed in Fig. 9. The dotted lines represent the linear regression curves. It shows that a clear straight line relationship is not observed for both the cases, but the shape of the plot seems to be very similar to that observed from the DMTA investigations in the temperature range of 30–80°C. This indicates that the change in temperature has a similar effect on the shift factors obtained by the two different methods, only the magnitude of a_T varies.

However the results overall indicate that the WLF equation is probably unsuitable for the PBT. This seems to arise from the semicrystalline nature, whose free volume can be thought to be quantized [35]. Therefore, it is expected to follow an Arrhenius type of relationship for the major transitions. When the shift factors of the DMTA investigations were plotted against inverse of temperature in Fig. 10 keeping the reference temperature same, it appears that the shift data can be better described in terms of the Arrhenius apparent activation energy (E) defined by the *Eq. 2*. It shows that the $\log a_T$ decreases with the rise in temperature. The linear regression curves are also

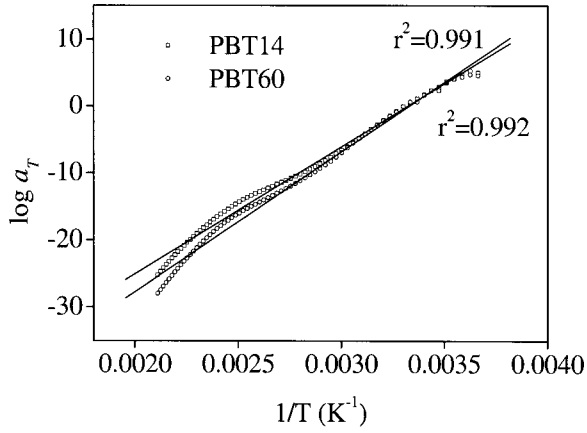

FIG. 10. Dependence of shift factor obtained from DMTA data on temperature; (——) represents first-order regression line.

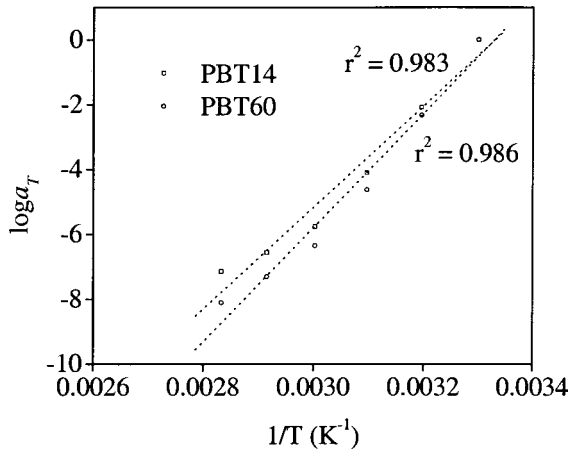

FIG. 11. Dependence of shift factor obtained from creep data on temperature; (· · · · ·) represents first-order regression line.

shown in the plot to calculate the activation energies of the deformation process. The apparent activation energies calculated from the slope of the regression curves were found to be 363 and 400 kJ/mol for PBT14 and PBT60, respectively. Values from 205–460 kJ/mol are reported elsewhere [36–39]. The larger the activation energy, the greater influence the change in temperature has on a_T. Higher activation energy for PBT processed at higher mold temperature can thus be explained from the higher shift of the individual storage modulus curves to the reference. The negative sign only indicates shifting to a reference at lower temperature and vice-versa. A number of studies utilizing nuclear magnetic resonance (NMR) C-13, chemical shift anisotropy and dielectric response revealed that the nature of molecular motions in PBT varies with the degree of crystallinity [37–40]. However a detailed investigation in this regard is beyond the scope of the present study and has therefore been skipped.

Figure 11 shows the plot of shift factors obtained from the flexural creep data against inverse of temperature (at same reference temperature). It is clear that the shift data can be better described by the Arrhenius model than the WLF model indicated by their regression factor. The activation energies calculated from the slope of the regression curves were found to be 299 and 337 kJ/mol for PBT molded at 14 and 60°C, respectively. The creep tests showed lower activation energies for both the PBTs which can be attributed to the difference in the deformation process involved in the two test methods.

CONCLUSION

Variation of the mold temperature showed a significant effect on the long-term viscoelastic behavior of the injection-molded PBT. The stiffness of the material is enhanced and creeping is reduced by increasing the mold temperature. This could be attributed to the slower cooling experienced by the specimens while processing at higher mold temperature that resulted in higher crystallinity as well as higher molecular packing in the molded parts. Applying four-element Burger model to the creep data, a constitutive representation of the creep behavior of PBT injection moldings could be made. The model analysis indicated that elastic and retardant modulus as well as the viscosity increased with the increase in the molding temperature that reduced creeping. The modeling parameters provided better understanding of the structure-to-property relationship when the mold temperature was varied. The TTS principle was applied to the DMTA and flexural creep data and shift factors were compared with Arrhenius and WLF equations. It was found that an Arrhenius type relaxation model held well for PBT processed at both the mold temperatures. Based on Arrhenius equation, the activation energies were calculated. Higher activation energy was manifested for PBT processed at higher mold temperature, which could be attributed to the higher energy associated with the deformation process.

ACKNOWLEDGMENTS

The authors thank BASF, Germany, for their cost-free supply of the material. Thanks are also due to Mr. Helmut Pueschner of the Institute of Mechanical and Plastics Engineering (Chemnitz University of Technology) for his technical assistance during injection molding.

REFERENCES

1. S. Fakirov, *Handbook of Thermoplastic Polyesters, Vol. 1*. Wiley-VCH Press, Weinheim (2002).
2. R. Jakeways, M.A. Wilding, I.M. Ward, I.H. Hall, I.J. Desborough, and M.G. Pass, *J. Polym. Sci. Polym. Phys. Ed.*, **13**, 799 (1975).
3. A.A. Apostolov, S. Fakirov, M. Pavlov, and N. Stribeck, *J. Mater. Sci. Lett.*, **21**, 145 (2002).
4. M.L.D. Lorenzo and M.C. Righetti, *Polym. Bull.*, **53**, 53 (2004).
5. G.L. Wilkes and C.M. Chu, *J. Appl. Polym. Sci.*, **18**, 2221 (1974).
6. M.P. Van der Wielen, *Polym. Eng. Sci.*, **15**, 17 (I975).
7. M. Yokouchi, Y. Sakakibara, Y. Chatani, H. Tadokoro, T. Tanaka, and K. Yoda, *Macromolecules*, **9**, 266 (1986).
8. M.G. Brereton, G.R. Davies, R. Jakeways, T. Smith, and I.M. Ward, *Polymer*, **19**, 17 (1978).
9. K. Tashiro, Y. Nakai, M. Kobayashi, and H. Tadokoro, *Macromolecules*, **9**, 137 (1980).
10. G. Farrow, J. McIntosh, and I.M. Ward, *Makromol. Chem.*, **38**, 147 (1960).
11. E.P. Chang and E.L. Slagowski, *J. Appl. Polym. Sci.*, **22**, 769 (1978).
12. K. Banik and G. Mennig, *Polym. Eng. Sci.*, **46**, 882 (2006).
13. K. Banik and G. Mennig, *Mech. Time-Dependent Mater.*, **9**, 247 (2006).
14. L.E. Nielsen, *Dynamic Mechanical Testing, Mechanical Properties of Polymers*, Van Nostrand Reinhold, New York (1962).

 DOI 10.1002/pen

15. W.F.H. Borman, *Polym. Eng. Sci.*, **22**, 883 (1982).
16. H.-J. Ludwig and P. Eyerer, *Polym. Eng. Sci.*, **28**, 143 (1988).
17. S. Houshyar, R.A. Shanks, and A. Hodzic, *Polym. Test.*, **24**, 257 (2005).
18. S. Houshyar and R.A. Shanks, *J. Appl. Polym. Sci.*, **105**, 390 (2007).
19. J.K. DePorter, D.G. Baird, and G.L. Wilkes, *J. Macromol. Sci. Part C: Rev. Macromol. Chem. Phys.*, **C33**, 1 (1993).
20. J.D. Ferry, *Viscoelastic Properties of Polymers*, *2nd ed.*, Wiley, New York (1970).
21. R.P. Chartoff, "Thermoanalytical Instrumentation, Techniques, and Methodology," in *Thermoplastic Polymers*, *2nd ed.*, E.A. Turi, Ed., Academic Press, San Diego (1997).
22. M.L. William, R.F. Landel, and J. Ferry, *J. Am. Chem. Soc.*, **77**, 3701 (1955).
23. W.N. Findley, J.S. Lai, and K. Onaran, *Creep and Relaxation of Nonlinear Viscoelastic Materials—With an Introduction to Linear Viscoelasticity*, Dover, New York (1976).
24. A.J. Nuñez, N.E. Marcovich, and M.I. Arangueren, *Polym. Eng. Sci.*, **44**, 1594 (2004).
25. M. Moneke, Die Kristallisation von verstärkten Thermoplasten während der schnellen Abkühlung und unter Druck, Ph.D. Thesis, Technische Universität Darmstadt, Germany (2001).
26. L.C.E. Struik, *Physical Ageing in Amorphous Polymers and Other Materials*, Elsevier, Amsterdam (1978).
27. L.C.E. Struik, "Physical Ageing: Influence on the Deformation Behavior of Amorphous Polymers," in *Failure of Plastics*, W. Brostow and R.D. Corneliussen, Eds., Hanser, München (1986).
28. K. Engelsing, Einfluβ des freien Volumens auf das verarbeitungsabhängige Deformationsverhalten spritzgegossener amorpher Thermoplaste, Ph.D. Thesis, Technische Universität Chemnitz, Germany (2000).
29. K.H. Illers and H. Breuer, *J. Coll. Sci.*, **18**, 1 (1963).
30. T.A. Osswald and G. Menges, *Materials Science of Polymers for Engineers*, Hanser, Munich (1996).
31. K.P. Menard, *Dynamic Mechanical Analysis*, CRC Press, Florida (1991).
32. R. Mark and W.N. Findley, *J. Rheol.*, **22**, 471 (1978).
33. C. Marias and G. Villoutreix, *J. Appl. Polym. Sci.*, **69**, 1983 (1998).
34. D. Feng, D.F. Caulfield, and A.R. Sanadi, *Polym. Compos.*, **22**, 506 (2001).
35. N. Dutta and G.H. Edward, *J. Appl. Polym. Sci.*, **66**, 1101 (1997).
36. W.P. Leung and C.L. Choy, *J. Appl. Polym. Sci.*, **27**, 2693 (1982).
37. G.J. Pratt and M.J.A. Smith, *J. Mater. Sci.*, **25**, 477 (1990).
38. E. Dobrovolny-Marand, S.L. Hsu, and C.K. Shih, *Macromolecules*, **20**, 1022 (1987).
39. L.W. Jelinski, J.J. Dumais, and A.K. Engel, *Macromolecules*, **16**, 403 (1983).
40. L.W. Jelinski and J.J. Dumais, *Polym. Prepr. (Am. Chem. Soc. Div. Polym. Chem.)*, **22**, 273 (1981).